

PAPER

Controlling direct contact force for wet adhesion with different wedged film stabilities

To cite this article: Meng Li *et al* 2018 *J. Phys. D: Appl. Phys.* **51** 165305

View the [article online](#) for updates and enhancements.

Related content

- [Topical Review](#)
Cosima Stubenrauch and Regine von Klitzing
- [Dewetting at the interface between two immiscible polymers](#)
G Krausch
- [Particle contact angles at fluid interfaces: pushing the boundary beyond hard uniform spherical colloids](#)
Michele Zanini and Lucio Isa

Controlling direct contact force for wet adhesion with different wedged film stabilities

Meng Li¹, Jun Xie¹, Liping Shi^{1,2}, Wei Huang¹ and Xiaolei Wang¹ 

¹ College of Mechanical & Electrical Engineering, Nanjing University of Aeronautics & Astronautics, Nanjing 210016, People's Republic of China

² College of Mechanical Engineering, Anhui University of Technology, Ma'anshan 243002, People's Republic of China

E-mail: wxl@nuaa.edu.cn

Received 28 December 2017, revised 1 March 2018

Accepted for publication 9 March 2018

Published 3 April 2018



CrossMark

Abstract

In solid–liquid–solid adhesive systems, wedged films often feature instability at microscopic thicknesses, which can easily disrupt the adhesive strength of their remarkable direct contact force. Here, sodium dodecyl sulfate (SDS) was employed to tune the instability of adhesion in wedged glass–water–rubber films, achieving controllable direct contact. Experimental results showed that the supplement of SDS molecules significantly weakened the direct contact force for wet adhesion and eliminated it at high concentrations. The underlying reason was suggested to be the repulsive double-layer force caused by SDS molecules, which lowers the instability of the wedged film and balances the preload, disrupting the direct contact in wet adhesion.

Keywords: sodium dodecyl sulfate, wet adhesion, direct contact force, wedged film, instability, dewetting

(Some figures may appear in colour only in the online journal)

1. Introduction

The adhesion of two surfaces under wet conditions is of crucial interest for many practical applications in our daily life and the biological world. When driving on a rainy day, a strong adherence to wet roads is desirable if one wants to keep the car under control. In the rainforest, certain amphibians—such as tree frogs, newts etc—utilize the reliable adhesive abilities of such surfaces to help them cling to the wet leaves or stones of their habitat [1–3]. In comparison to dry adhesion systems, intercalation of a liquid film between contacts greatly complicates understanding of the adhesion behavior due to the drastic liquid–solid interaction [4–8].

Recently, various studies carried out on polydimethylsiloxane (PDMS) surfaces to simulate the remarkable wet adhesion of amphibians have demonstrated that solid–liquid interactions make a great contribution to surface adhesive performance [6, 7, 9, 10]. For example, adhesion measured on PDMS with water presented a significant force, comprising

direct contact and capillary contributions [6, 11]. By contrast, for a plasma treated PDMS, the wet adhesion force was dominated by only capillary interactions, with a weakened overall value [6]. According to previous studies by Martin *et al* [12–14], the direct contact force for wet adhesion is a result of dewetting behavior due to the unstable film wedged between probe and PDMS. The behavior depends on the sign of the spreading parameter S ($S = \gamma_{SR} - (\gamma_{SL} + \gamma_{LR})$, where γ_{ij} are the solid/rubber, solid/liquid, and liquid/rubber interfacial tensions) which compares interfacial energies between ‘dry’ contacts γ_{SR} and lubricated contacts $\gamma_{SL} + \gamma_{LR}$ [14–16]. If S is positive, the wedged film is stable and performs as an interlayer. However, if S is negative, the wedged film is unstable, and easily collapses for direct contacts under thinning by a preload. Moreover, compared with films exposed to air, a wedged one is less fragile at the same metastable thickness [14, 17]. The dewetting only occurs for very thin films, often reaching the unstable thickness (1 μm) at which it dewets spontaneously [17–21].

Various studies have focused on the withdrawal behavior of liquid films sandwiched between solids and rubbers during the dewetting process [14, 17, 19, 21–24]. However, from an adhesive point of view, designing interfacial properties and achieving a tunable adhesive strength seems more interesting for scientists. A well-known—and the best studied—example is that of controlling dry adhesion with topographic patterns [25, 26]. For solid–liquid–solid systems, the above proposed mechanisms of collapse of the wedged film also suggest the possibility of tuning adhesion via the controllable direct contact force. Unfortunately, little research has so far been conducted to comprehend the effect on direct contact force for wet adhesion of varying inclinations to collapse, i.e. instabilities, of wedged films.

In this paper, SDS molecules have been employed to achieve varying stabilities of wedged films in glass(probe)–water–rubber (PDMS) systems. Wet adhesion experiments were then performed to study the direct contact effect in these various wedged films. Meanwhile, energetics models were set up to theoretically analyze and discuss the mechanism of collapse of water films and the effect of SDS on film dewetting in adhesion.

2. Experimental details

2.1. Sample fabrication

PDMS (Sylgard 184, Dow Corning) was mixed with a prepolymer-to-cross-linker ratio of 10:1, poured into a prepared glass mold, and degassed in a desiccator. The filled mold was then placed in an oven and cured at 75 °C for 4 h. After cooling to room temperature, the PDMS sample was carefully peeled from the mold.

2.2. Wet adhesion measurements

Wet adhesion measurements were performed using a custom-made setup, shown in figure 1(a), which is also described in detail in [11]. The probe used here is a plano-convex lens with a curve radius of 18.5 mm (Purshee, China), Young's modulus of 7.2×10^{11} Pa and Poisson's ratio of 0.2. Solutions with a range of SDS content (m/m%) were selected to achieve varied wedged film stabilities on PDMS for adhesion. The surface tension of SDS solutions and their contact angles on PDMS are shown in figure 2(a). An aliquot of 3 μl was first placed on the PDMS surface using a micropipette and located at the center of the probe under the microscope. Measurements were then performed with the probe approaching, indenting, static and retracting, and the specific progress was graphically shown in figure 1(b). Represent force–distance curves measured with water and SDS solution (0.05%) are shown in figures 2(b) and (c). The preload was 2 mN and the standing time 5 s. For retractions, the piezo first moved at a speed of 1 $\mu\text{m s}^{-1}$ to conduct the short-range detachment; beyond the piezo range (100 μm), a step motor was activated at the speed of 10 $\mu\text{m s}^{-1}$ to break the long-range capillary interaction. The whole measurement process was recorded via force

sensor and monitored using an optical camera. Each sample was tested at least five times.

3. Results and discussion

3.1. The content of SDS controlled direct contact for wet adhesion

Figure 3(a) shows the wet adhesion forces measured on flat PDMS in the presence of solutions with various concentrations of SDS. It can be seen that in the water case (0.00% content of SDS), the wet adhesion force shows its highest value of about 22.52 mN, but the addition of SDS strongly weakens it. The lowest wet adhesion force was found at the maximum content of SDS (0.05%)—about 5.82 mN. Moreover, from the raw force–distance curves in figures 2(b) and (c), one can easily find that the detachment in the water case has two distinct contributions: the short-range direct contact force and long-range capillary force (see [27] for detailed discussion), but for 0.05% SDS solution, only the capillary force contributes. This suggests that the wedged water between the probe and PDMS is unstable under preloading, and finally dewets for direct contacts, achieving a remarkable adhesion force. However, for the solution with highest SDS concentration, the wedged film is always stable, separating the probe and PDMS and causing a weak capillary adhesion. The *in situ* microscopic detachments of the probe from the PDMS shown in figure 4 further confirm this. The direct contact was clear and easily observed in water (0.00% content), but could not be found in 0.05% SDS solution.

Figure 4 also indicates a visual transformation from dewetting (unstable) to wetting (stable) for films wedged between the probe and PDMS with increased content of SDS. To reveal the nature of this transformation quantitatively, the data of figure 3(a) were divided into two parts—direct contact and capillary contribution—as shown in figure 3(b), based on their separate behaviors in force–distance curves. It can be found that the capillary force changes slightly with varying content of SDS, but for direct contact force, it decreases strongly with the increase in SDS content. This suggests that the weakened wet adhesion of SDS solution (figure 3(a)) is a result of decreased direct contact force, and the SDS can reduce the instability of wedged film, weakening the dewetting for a direct contact.

3.2. Why can SDS reduce the direct contact contribution for wet adhesion?

3.2.1. The collapse of water. Early studies by Roberts *et al* have reported the spontaneous collapse of distilled water between rubber and glass; the critical thickness is about 400 Å [18]. Later, Martin *et al* pointed out that the collapse of direct contact in wedged films is a dewetting behavior of unstable liquids, controlled by the spreading coefficient $S = \gamma_{\text{SR}} - (\gamma_{\text{SL}} + \gamma_{\text{RL}}) = S^{\text{LW}} + S^{\text{P}}$, where γ_{ij} are the solid (probe)/rubber (PDMS), solid (probe)/liquid and rubber/liquid components, respectively, of the spreading

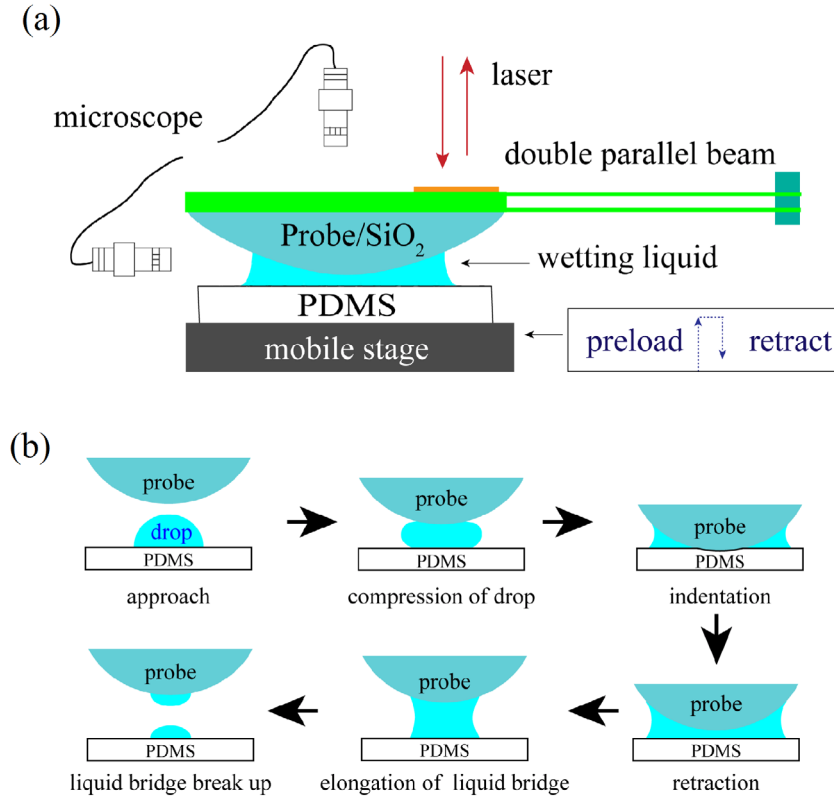


Figure 1. (a) Schematic illustration of the measurement setup, (b) specific progress of wet adhesion measurement.

coefficient and S^{LW} and S^P are its Lifshitz–van der Waals and polar components [28, 29]. If $S < 0$, it is capable of dewetting for direct contacts with two regimes, metastable and unstable, depending on film thickness.

To reveal the mechanism behind the transformation for SDS solution from unstable to stable, the free energy function F of the wedged film versus its thickness e should be determined. Referring to previous studies [30–32], the F for wedged water from macro to micro scale can be expressed as

$$F(e) = \gamma_{SL} + \gamma_{RL} + P(e)^{LW} + P(e)^P + \frac{1}{2}\rho g e^2, \quad (1)$$

where $P(e)^{LW}$ is the long-range contribution of Lifshitz–van der Waals, $P(e)^P$ is short-range polar contribution, ρ is liquid density, g is acceleration due to gravity. The $P(e)^{LW}$ and $P(e)^P$ can be described as follows [15, 23, 33]:

$$\begin{cases} P(e)^{LW} = -\frac{A}{12\pi e^2} \\ P(e)^P = S^P \exp[(a - e)/l] \end{cases}, a \ll e \quad (2)$$

$$\begin{cases} P(e \rightarrow 0)^P = P(e = a)^P = S^P \\ P(e \rightarrow 0)^{LW} = S^{LW} \end{cases}, \quad (3)$$

where A is the effective Hamaker constant (which can be expressed by $A = A_L + A_{SR} - A_{RL} - A_{SL}$), a is the size of a liquid molecule, and l is the correlation length for the polar fluid. For water, l appears to be in the range of 0.2 and 1 nm, and an estimate of the best value is about 0.6 nm [15], S^P is $-2\gamma_L^P$ [34]. Thus, equation (1) can be written as

$$F(e) = \gamma_{SL} + \gamma_{RL} - \frac{A}{12\pi e^2} - 2\gamma_L^P \exp[(a - e)/l] + \frac{1}{2}\rho g e^2. \quad (4)$$

When $e \rightarrow 0$, the $F(e)$ is γ_{SR} : the water molecules are squeezed out and glass directly contacts with the PDMS substrate.

Similarly to films exposed to air [31, 33], the free energy of wedged water $F(e)$ can be qualitatively studied based on properties of formula components, as shown in figure 5. It can be seen that if the spreading S is negative, the free energy $F(e)$ decreases with the decreased film thickness e , and there is a critical thickness e_c ($\ll 1 \mu\text{m}$) at which the second derivative $F''(e) = 0$. For mesoscopic films ($e > e_c$), the curvature of $F(e)$ is positive ($F''(e) > 0$), the wedged film is metastable, and dewetting requires nucleation at a single contact point. However, for a wedged film, this kind of dewetting for direct contact is not easy [17]. For nanoscopic films ($e < e_c$), the curvature of $F(e)$ is negative ($F''(e) < 0$), the wedged film is unstable and dewets spontaneously. When water was wedged between glass and PDMS, the film thinned heavily under a preload, easily reaching e_c . Therefore, a spontaneous-collapse-induced direct contact usually occurs in water adhesion.

3.2.2. The SDS effect on water collapse. On the addition of SDS to the water, the tendency of the wedged film to collapse weakened and vanished. The direct contact force was also eliminated in the constrained thin film. To reveal these characteristics, a free energy model was also set up. Early papers have proved that there was an electrical double-layer repulsive force caused by SDS ions in the sandwiched system

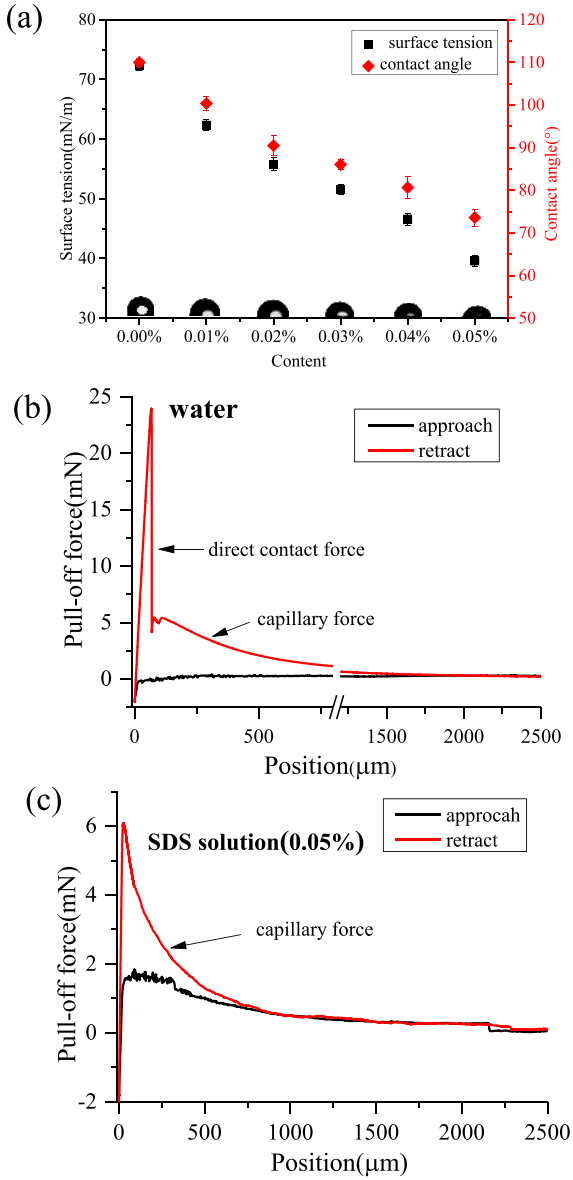


Figure 2. (a) Surface tensions of SDS solutions and their contact angles on PDMS surface, (b) force–distance curves measured on PDMS surface in the presence of water and (c) SDS solution (0.05%).

[18, 35–37]. Hence, our model considers the potential energy of electrical repulsion; it was expressed as

$$F(e) = \gamma_{SL} + \gamma_{RL} - \frac{A}{12\pi e^2} - 2\gamma_L^p \exp[(a - e)/l] + \frac{1}{2} \rho g e^2 + \frac{k}{2\pi} Z \exp(-ke). \quad (5)$$

Here, k^{-1} is the Debye length; Z is an interaction constant, which is analogous to the Hamaker constant A . Noted that the interaction constant Z is defined in terms of the surface potential of the isolated surfaces (at $e = \infty$), but it can also be expressed in terms of the surface charge density by applying the Grahame equation [38]. Therefore, here it is a parameter that is related to the content of SDS. In addition to the

repulsive force, the addition of SDS also reduces the probe–liquid and PDMS–liquid interfacial tension. For convenience, equation (5) was analyzed using a control variate method.

3.2.2.1. The influence of solid–liquid interfacial energy. Figure 6 shows the decrease of solid–liquid interfacial tension caused by SDS in the free energy curve $F(e)$. The glass–PDMS interfacial energy is fixed as a constant. The decreased contribution of the interfacial energy $\gamma_{SL} + \gamma_{RL}$ lowers the free energy curve of $F(e)$ and the absolute value of spreading coefficient S decreases significantly. However, because the contact angles between the SDS solution and PDMS range from 110° to 74° , they are configured in a partial wetting case, as shown in figure 2(a). Therefore, the spreading coefficient is still negative and its direction is still downward, or the $\gamma_{SL} + \gamma_{RL}$ cannot fall below the interfacial energy of glass–PDMS (γ_{SR}). It is still capable of dewetting for direct contact. Moreover, because of the nearly parallel translation of function curve, the second derivative of $F(e)$ is still negative ($F''(e) < 0$) when $e < e_c$. Thus, if the wedged film thins down under a preload, dewetting will still occur for direct contact. The decreased glass–liquid and PDMS–liquid interfacial energy caused by SDS molecules is not the key factor of the decreased contact force in wet adhesion (figure 3(b)). It should be noted that the SDS may also decrease the coefficient of polar interaction $-2\gamma_L^p$ (equation (5)), but this change does not affect the spreading coefficient S or change the negative sign of the second derivative of $F(e)$.

3.2.2.2. The influence of electrical double-layer repulsion. Figure 7 shows the influence of electrical double-layer repulsion caused by SDS on the free energy curve of $F(e)$. The dark line represents the $F(e)$ of wedged water; the colorized ones represent those of wedged SDS solutions. The combined effect of van der Waals (VDW) forces and electrical double-layer imposes an interaction energy similar to Derjugin–Landau–Verwey–Overbeek (DLVO) theory [39]. During thinning due to preloading, the electrical double-layer repulsion for SDS solution prevents contact between the upper and lower solid–liquid interfaces. Unlike the VDW interaction, this repulsion effect produces a potential energy in the wedged film. The sign of Z in equation (5) depends on the surface charge density, which is related to SDS molecule concentration. The higher the SDS concentration is the stronger the electrical repulsion and potential energy become. Sufficient electrical repulsion gives the curve of free energy versus film thickness a concave shape (dashed line in figure 7) at the microscale—most obviously for the red line. This leads to a smaller critical thickness e_c for the unstable film in comparison to the dark line, whose free energy was dominated only by polar and VDW interaction. Note that at the critical thickness $e_c(F''(e) = 0)$, this means that the repulsive resultant force, i.e. the first derivative $F'(e)$, for the whole system reaches a maximum. In an SDS solution for wet adhesion, if the preload can be balanced by that repulsive force (the preload \leq the maximum of $F'(e)$), the thinning thickness of the wedged film cannot reach the unstable value

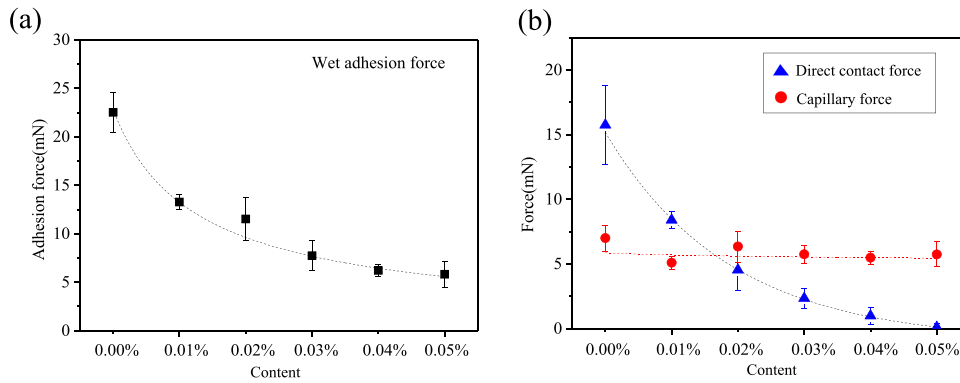


Figure 3. (a) Wet adhesion force measured on PDMS in the presence of varying SDS solutions, (b) the direct contact and capillary force contribution in wet adhesion with varying SDS solution.

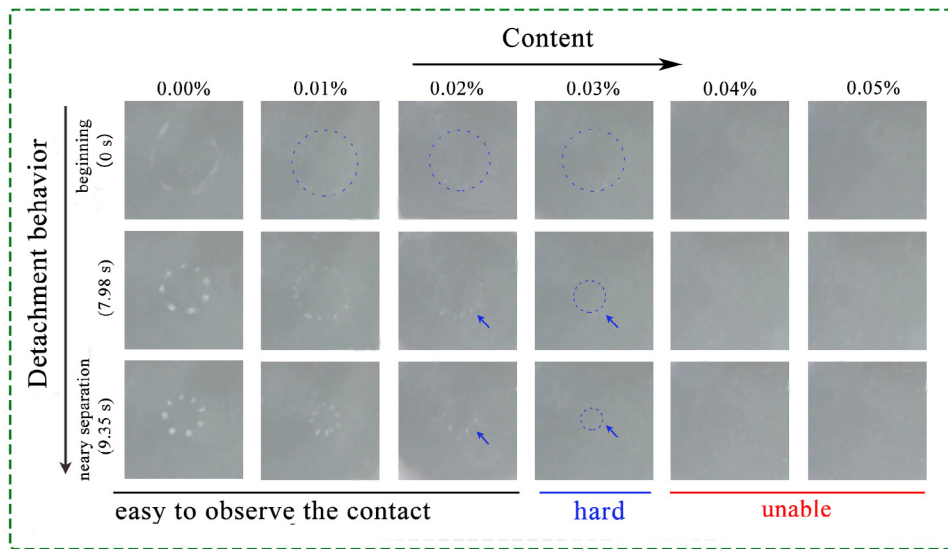


Figure 4. Optical microscope pictures of detached behavior between probe and PDMS during adhesion measurements.

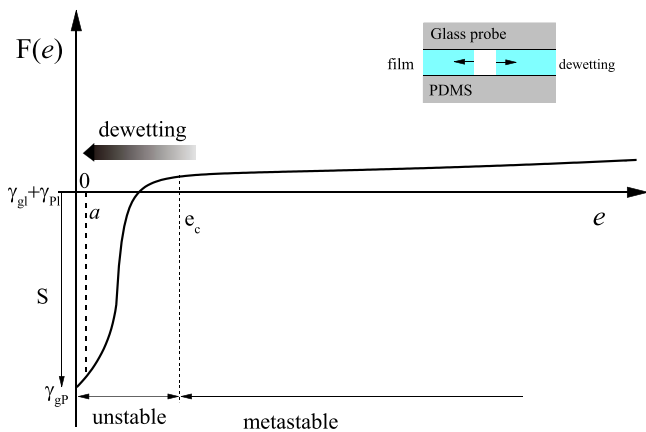


Figure 5. Free energy F of wedged water versus film thickness e .

$e_c(F''(e) = 0)$. Therefore, the dewetting necessary for direct contact force will not happen at high concentrations of SDS solution—for example, the content of 0.05% in figure 3(b).

For low concentrations of SDS, the dewetting of the wedged film still happens because of the insufficiently repulsive effect. The decrease of direct contact force with the content from 0.00% to 0.04% in figure 3(b) may be due to the

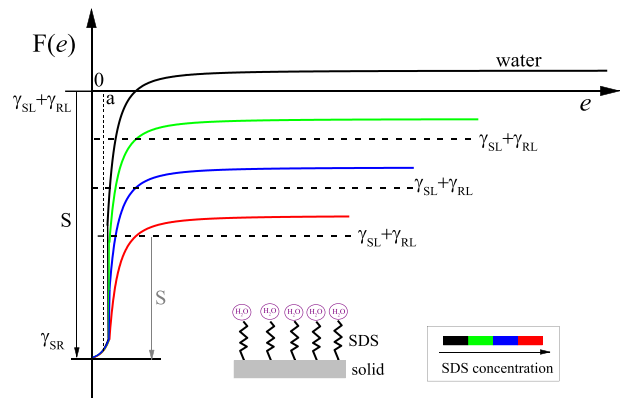


Figure 6. The influence of interfacial tension on free energy $F(e)$.

decreased contact area. As the spherical probe surface indents the PDMS, it leaves a crack whose thickness varies from the center of contact to the exterior. When the wedged film collapses, the direct contact radius is from the contact center to a place in the crack at which the film has the critical thickness e_c . Hence, the high concentration of SDS leads to a small contact area and a low direct contact force for wet adhesion.

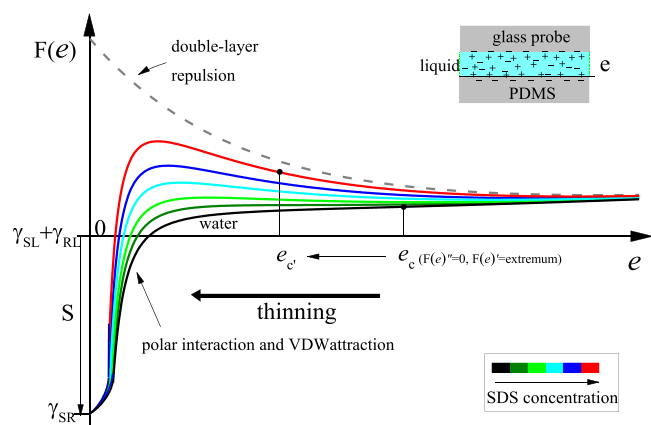


Figure 7. The influence of electrical double-layer repulsion on free energy $F(e)$.

4. Conclusion

In this paper, we have employed SDS molecules to tune the instability of a glass-water-rubber wedged film system, to achieve controllable direct contact for wet adhesion. The experimental tests demonstrate that the SDS molecules weaken the tendency of the wedged film to collapse, and the direct contact force in wet adhesion decreases strongly with increased SDS concentration. Energetic models were set up for theoretical analyses. The results suggest that it is not the decrease of liquid surface energy but the supplement of electrical double-layer repulsion caused by the SDS which prevents the collapse of wedged films and decreases the direct contact force in wet adhesion. These findings have important implications for the development of new reversible adhesives for wet conditions.

Acknowledgments

This research was supported by the National Nature Science Foundation of China (NSFC) (Grant No. 51675268), the Fundamental Research Funds for the Central Universities (Grant NZ2016106) and Natural Science Foundation of Anhui Province of China (1708085QE113).

ORCID iDs

Xiaolei Wang  <https://orcid.org/0000-0002-9055-1011>

References

- [1] Hanna G and Barnes W J P 1991 Adhesion and detachment of the toe pads of tree frogs *J. Exp. Biol.* **155** 103–25
- [2] Barnes W J P 2007 Functional morphology and design constraints of smooth adhesive pads *MRS Bull.* **32** 479–85
- [3] Huang W and Wang X L 2013 Biomimetic design of elastomer surface pattern for friction control under wet conditions *Bioinspir. Biomim.* **8** 046001
- [4] Wang S, Li M, Huang W and Wang X 2016 Sticking/climbing ability and morphology studies of the toe pads of Chinese fire belly newt *J. Bionic Eng.* **13** 115–23
- [5] Roshan R, Jayne D G, Liskiewicz T, Taylor G W, Gaskell P H, Chen L, Montellano-Lopez A, Morina A and Neville A 2011 Effect of tribological factors on wet adhesion of a microstructured surface to peritoneal tissue *Acta Biomater.* **7** 4007–17
- [6] Drotlef D M, Stepien L, Kappl M, Barnes W J P, Butt H J and del Campo A 2013 Insights into the adhesive mechanisms of tree frogs using artificial mimics *Adv. Funct. Mater.* **23** 1137–46
- [7] Iturri J, Xue L, Kappl M, García-Fernández L, Barnes W J P, Butt H J and del Campo A 2015 Torrent frog-inspired adhesives: attachment to flooded surfaces *Adv. Funct. Mater.* **25** 1499–505
- [8] Federle W, Barnes W J, Baumgartner W, Drechsler P and Smith J M 2006 Wet but not slippery: boundary friction in tree frog adhesive toe pads *J. R. Soc. Interface* **3** 689–97
- [9] Li M, Huang W and Wang X 2015 Bioinspired, peg-studded hexagonal patterns for wetting and friction *Biointerphases* **10** 031008
- [10] Chen H, Zhang L, Zhang D, Zhang P and Han Z 2015 Bioinspired surface for surgical graspers based on the strong wet friction of tree frog toe pads *ACS Appl. Mater. Inter.* **7** 13987–95
- [11] Li M, Huang W and Wang X 2017 Advanced adhesion and friction measurement system *Meas. Sci. Technol.* **28** 035601
- [12] Martin P, Silberzan A P and Brochardwyart F 1997 Sessile droplets at a solid/elastomer interface *Langmuir* **13** 4910–4
- [13] Martin P 1998 Adhesion of a soft rubber on a wet solid *J. Adhes.* **67** 139–51
- [14] Martin P and Brochard-Wyart F 1998 Dewetting at soft interfaces *Phys. Rev. Lett.* **80** 3296–9
- [15] Sharma A 1993 Relationship of thin film stability and morphology to macroscopic parameters of wetting in the apolar and polar systems *Langmuir* **9** 861–9
- [16] Wyart F B and Daillant J 1989 Drying of solids wetted by thin liquid films *Can. J. Phys.* **68** 1084–8
- [17] Martin A, Buguin A and Brochardwyart F 2001 Dewetting nucleation centers at soft interfaces *Langmuir* **17** 6553–9
- [18] Roberts A D and Tabor D 1968 Surface forces: direct measurement of repulsive forces due to electrical double layers on solids *Nature* **219** 1122
- [19] Brochardwyart F and Gennes P G D 1994 Dewetting of a water film between a solid and a rubber *J. Phys. Condens. Matter* **6** A9
- [20] Reiter G, Sharma A, Casoli A, David M O, Khanna R and Auroy P 1999 Destabilising effect of long-range forces in thin liquid films on wettable substrates *Europhys. Lett.* **46** 512
- [21] Brochardwyart F, Buguin A, Martin P, Martin A and Sandre O 2000 Adhesion of soft objects on wet substrates *J. Phys. Condens. Matter* **12** A239–44
- [22] Sharma A and Reiter G 1996 Instability of thin polymer films on coated substrates: rupture, dewetting, and drop formation *J. Colloid Interface Sci.* **178** 383–99
- [23] Sharma A, Casoli A, David M, Khanna R and Auroy P 1999 Thin film instability induced by long-range forces *Langmuir* **15** 2551–8
- [24] Martin A, Rossier O, Buguin A, Auroy P and Brochard-Wyart F 2000 Spinodal dewetting of thin liquid films at soft interfaces *Eur. Phys. J. E* **3** 337–41
- [25] Sameoto D and Menon C 2010 Recent advances in the fabrication and adhesion testing of biomimetic dry adhesives *Smart Mater. Struct.* **19** 103001
- [26] Kamperman M, Kroner E, del Campo A, McMeeking R M and Arzt E 2010 Functional adhesive surfaces with ‘Gecko’ effect: the concept of contact splitting *Adv. Eng. Mater.* **12** 335–48
- [27] Li M, Xie J, Dai Q, Huang W and Wang X 2018 Effect of wetting case and softness on adhesion of bioinspired

- micropatterned surfaces *J. Mech. Behav. Biomed. Mater.* **78** 266–72
- [28] Oss C J V, Good R J and Chaudhury M K 1988 Additive and nonadditive surface tension components and the interpretation of contact angles *Langmuir* **4** 884–91
- [29] van Oss C J, Chaudhury M K and Good R J 1987 Monopolar surfaces *Adv. Colloid Interface Sci.* **28** 35–64
- [30] Brochardwyart F, Meglio J M D, Quere D and Gennes P G D 1991 Spreading of nonvolatile liquids in a continuum picture *Langmuir* **7** 335–8
- [31] Redon C, Brochard-Wyart F and Rondelez F 1991 Dynamics of dewetting *Phys. Rev. Lett.* **66** 715–8
- [32] Wyart F B, Martin P and Redon C 1993 Liquid/liquid dewetting *Langmuir* **9** 3682–90
- [33] Sharma A 1993 Equilibrium contact angles and film thicknesses in the apolar and polar systems: role of intermolecular interactions in coexistence of drops with thin films *Langmuir* **9** 3580–6
- [34] Khanna R, Jameel A T and Sharma A 1996 Stability and breakup of thin polar films on coated substrates: relationship to macroscopic parameters of wetting *Ind. Eng. Chem. Res.* **35** 3081–92
- [35] Roberts A D and Swales P D 1969 The elastohydrodynamic lubrication of a highly elastic cylindrical surface *J. Phys. D: Appl. Phys.* **2** 1317–26
- [36] Roberts A 1971 Role of electrical repulsive forces in synovial fluid *Nature* **231** 434–6
- [37] Roberts A D 1971 The shear of thin liquid films *J. Phys. D: Appl. Phys.* **4** 433
- [38] Israelachvili J N 1985 *Intermolecular and Surface Forces—Intermolecular and Surface Forces* 3rd edn (New York: Academic)
- [39] Marshall K C, Stout R and Mitchell R 1971 Mechanism of initial event in sorption of marine bacteria to surfaces *J. Gen. Microbiol.* **68** 337–48